AJNR

Development of an Ultrasound Scoring System to Describe Brain Maturation in Preterm Infants

A. Stein, E. Sody, N. Bruns and U. Felderhoff-Müser

Development of an Ultrasound Scoring System to Describe Brain Maturation in Preterm Infants

A. Stein, E. Sody, N. Bruns, and U. Felderhoff-Müser

ABSTRACT

BACKGROUND AND PURPOSE: Cerebral maturation in preterm infants predominantly occurs postnatally, necessitating the development of objective bedside markers to monitor this process. This study aimed to develop a straightforward objective Ultrasound Score of Brain Development to assess cortical development in preterm infants.

MATERIALS AND METHODS: A total of 344 serial ultrasound examinations from 94 preterm infants born at $\leq$ 32 weeks of gestation were analyzed to identify brain structures suitable for a scoring system.

RESULTS: Among 11 candidate structures, 3 cerebral landmarks were selected due to their correlation with gestational age: the interopercular opening ($P < .001$), the height of the insular cortex ($P < .001$), and the depth of the cingulate sulcus ($P < .001$). These structures can be easily visualized in a single midcoronal view in the plane through the third ventricle and the foramina of Monro. A score point from 0 to 2 was assigned to each measurement, culminating in a total score ranging from 0 to 6. The Ultrasound Score of Brain Development correlated significantly with gestational age ($P < .001$).

CONCLUSIONS: The proposed Ultrasound Score of Brain Development has the potential for application as an objective indicator of brain maturation in correlation with gestational age, circumventing the need to rely on individual growth trajectories and percentiles for each specific structure.

ABBREVIATIONS: β = regression coefficient; DOL = day or days of life; J = Youden index; PMA = postmenstrual age; ROC = receiver operating characteristic; SD = standard deviation; USBD = Ultrasound Score of Brain Development

Cerebral ultrasound in premature infants is a well-established bedside technique and is suitable for serial noninvasive and cost-effective examinations in clinical routine. Existing prenatal[1-6] and postnatal ultrasound[7-14] studies as well as MR imaging studies[15,16] have described postnatal brain development using growth trajectories of cerebellar diameter, corpus callosum length, and corpus callosum-fastigium length. To distinguish among different postmenstrual ages (PMAs), one should select anatomic structures that either exhibit significant developmental changes apart from growth or only appear at a later PMA. Fetal ultrasound studies[2,17-19] have established a well-defined temporal sequence of cortical sulcal development. Opercularization with formation of the Sylvian fissure as a 3D process has also been extensively described in prenatal ultrasound studies.[6,17-21]

Although several of these studies[7,18,19,22-24] proposed scoring systems, all studies used semiquantitative or pictorial approaches. Van der Knaap et al[23] suggested a scoring system to describe sulcal development from a V-shaped pit to a stage in which the sulcus is deeper than wide in a postnatal MR imaging study in neonates of >30 weeks' PMA. This score was adapted for intrauterine 2D and 3D ultrasound by Pistorius et al[18] and for postnatal MR imaging by Ruoss et al.[22] Postnatal standard transfontanellar ultrasound views differ from transabdominal axial prenatal views. Thus, Klebermass-Schrehof et al[7] used 3D techniques to adapt this score for postnatal ultrasound.

Our goal was to develop a practical and objective scoring system based on 2D assessment of cerebral anatomic structures in standard transfontanellar planes, which can be applied in routine serial postnatal ultrasound examinations to characterize postnatal brain development in accordance with PMA.

MATERIALS AND METHODS

Study Participants

In this retrospective study, 458 preterm infants born ≤32 + 0/ 7 weeks' PMA at the University Hospital Essen between May 2009
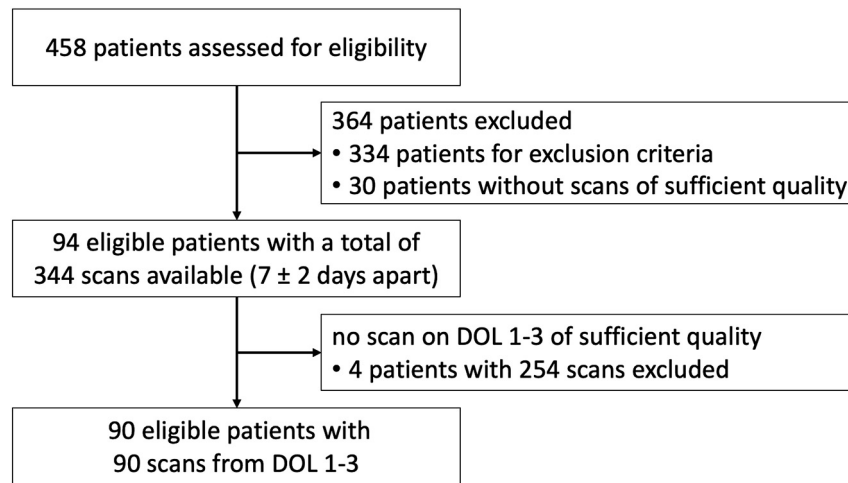
FIG 1. Flowchart of patient recruitment.

Table 1: Patient characteristics

Variable		Patients (*n* = 94)
Sex (No.)	Male	48
	Female	46
PMA at birth (weeks)[a]	Mean	27.8 (SD, 2.2)
	Range (min–max)	23 + 3/7 to 32 + 0/7
PMA at time of scan (weeks)	Mean	30.9 (SD, 3.4)
	Range (min–max)	23 + 4/7 to 39 + 1/7
Birth weight (g)	Mean	1034 (SD, 349)
	Range (min–max)	340–1810
Birth weight percentile	< 3rd (No.) (%)	3 (3.2%)
	3rd to 10th (No.) (%)	16 (17.0%)
Head circumference at birth (cm)	Mean	25.3 (SD, 2.7)
	Range (min–max)	18.4–31.0
Head circumference at birth percentile	< 3rd (No.) (%)	2 (2.1%)
	3rd to 10th (No.) (%)	21 (22.3%)

Note:—Min indicates minimum; max, maximum.
[a] PMA at birth was determined by ultrasound measurement of fetal crown rump length in the first trimester.

and September 2013 were eligible (Fig 1). We excluded 334 infants due to factors potentially influencing brain development, such as intraventricular or intracerebral hemorrhage, cystic periventricular leukomalacia, hydrocephalus, congenital infection, cerebral malformation, chromosomal or syndromal disorder, death during first hospital stay, or transfer to or from another clinic (outborn infants). The quality of archived ultrasound examinations was assessed on the basis of the correct identification of landmarks, symmetry of the required plane, and clear identification of the selected candidate structures. Scans from 30 infants were excluded because >2 of the selected cortical structures in all planes could not be identified and measured. To increase the number of scans and the range of PMAs, we included multiple scans of an individual patient if they were five to nine days apart, resulting in 344 cranial ultrasound examinations of 94 preterm infants (48 male, 46 female; mean birth weight = 1034 [SD, 349] g, range = 340–1810 g) for analysis with a range from 23 + 3/7 weeks at birth to a corrected age of 39 + 1/7 weeks. The total number of ultrasound scans per patient varied from 1 to 8.

The estimated date of delivery was determined by the obstetrician using an ultrasound measurement of crown rump length during first-trimester fetal ultrasound. Gestational age was confirmed

by fetal ultrasound at hospital admission for impending prematurity. There were no cases of unknown or uncertain gestational age in our cohort, but the accuracy of first-trimester dating varied from ±0.5 to ±1 weeks.

To exclude the potential influence of the postnatal clinical course on the results, we repeated the analysis by including only 1 scan per patient between the first and third days of life (DOL), which was available for 90 patients. Patient characteristics are summarized in Table 1.

Cranial Ultrasound
All cranial ultrasound examinations were conducted as part of a local routine monitoring protocol for preterm infants of ≤32 + 0/7 weeks PMA during the following timeframes: DOL 1, 3, 5, 7, 14 (±2 days), 21 (±2 days), and 28 (±2 days) and every 14 days (±2 days) thereafter until 36 + 0/7 weeks' PMA (±2 days). Additional examinations were performed as clinically indicated. Each examination was conducted by an experienced pediatrician as is standard in Germany, through the anterior fontanelle using a vector 7.5-MHz transducer (Acuson Sequoia 512; Siemens). Archived examinations were retrieved from magneto-optical discs and reopened on the ultrasound machine. A selection of 11 different candidate structures derived from previous studies on cortical development was identified and measured in the archived images in standard midsagittal and midcoronal planes (Fig 2). These planes are well-defined to allow reliable identification of the selected structures. Linear measurements of the height of the insular cortex were compared with measurements along the circumference (2 and 3 in Fig 2). A mean value was used for measurements of the same structure from the left and right hemispheres. Obviously asymmetric coronal images were excluded. The score was not designed to detect asymmetry in development.[18] All measurements were performed by a single observer blinded to the PMA.
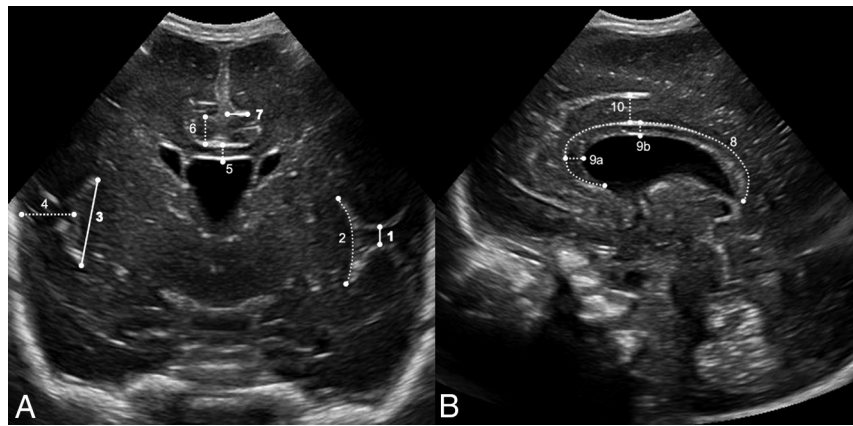
FIG 2. Ultrasound identification of the structures evaluated for the USBD in an infant with a PMA of 26 weeks. *A,* Midcoronal view at the level of the foramina of Monro: interopercular opening* (1), height of the insular cortex—curved measurement (2) and straight measurement* (3), depth of the Sylvian fissure (4), thickness of the corpus callosum (5), height of the cingulate gyrus (6), depth of cingulate sulcus* (7). *B,* Midsagittal view: circumferent length of corpus callosum (8), thickness of corpus callosum (midsagittal) at the genu (9a) and at the body (9b), and height of cingulate gyrus (10). *Asterisks* indicate structures selected for the USBD (*bold lines, A*).

Table 2: Linear regression analysis of the measured structure and PMA at time of scan

	No.	R	β	P Value
Interopercular opening[a]	343	−0.74	−0.06	<.001
Height of insular cortex, curved measurement	343	0.84	0.09	<.001
Height of insular cortex, straight measurement[a]	343	0.85	0.09	<.001
Depth of Sylvian fissure	341	0.19	0.06	<.001
Thickness of CC (midcoronal)	342	0.26	0.003	<.001
Height of cingulate gyrus (midcoronal)	313	0.72	0.06	<.001
Depth of cingulate sulcus[a]	315	0.83	0.05	<.001
Circumferent length of CC	311	0.68	0.17	<.001
Thickness of CC (midsagittal)				
Genu	335	0.32	0.01	<.001
Body	339	0.18	0.002	<.001
Height of cingulate gyrus (midsagittal)	260	0.44	0.02	<.001
Total USBD (all scans)	312	0.88	0.43	<.001
Total USBD (DOL 1–3)	87	0.76	0.41	<.001

Note:—No. indicates the number of scans in which the structure could be measured; CC, corpus callosum.
[a] Structures selected for the USBD.

Statistical Methods

Data analysis and graphic display generation were conducted using SPSS (release 28 for Mac; IBM) and Excel (release 16.53 for Mac; Microsoft). Linear regression of a selected cortical structure measurement with PMA was described by the Pearson correlation coefficient (R), regression coefficient (β), and 95% confidence interval. *P* values < .05 were considered statistically significant. Mean values, SDs, ranges, and interquartile ranges were used as appropriate. Regression curve analyses and receiver operating characteristic (ROC) curves with the Youden index (J) were used to identify and confirm cutoff values for the selected structures contributing to the score.

Development of the Ultrasound Score of Brain Development

The Ultrasound Score of Brain Development (USBD) aimed to discriminate among different PMAs using the state of cortical development. We sought to separate PMAs in 2-week increments by choosing staggered cutoff points for measurements of the selected structures. Structures were deemed suitable if

measurements demonstrated a clear progression in cortical development with a steep linear regression.

Ethics Approval

The study obtained approval from the local ethics committee of the University Duisburg-Essen (15–6268-BO).

RESULTS

Correlation of the 11 Candidate Structures with PMA

The thickness of the corpus callosum measured in the midcoronal view or at the body in the midsagittal view did not show a significant correlation with PMA when analyzing only scans from DOL 1–3. All other measurements correlated significantly with PMA (*P* < .001, Table 2), regardless of whether only scans from DOL 1–3 or all available scans were included. The curved and straight measurements of the insular cortex in the midcoronal view correlated equally well.

Development of the USBD

We selected 3 measurements with the highest correlation coefficients and steep regression curves for the score: the interopercular opening (R = 0.74), the height of the insular cortex (R = 0.85), and the depth of the cingulate sulcus (R = 0.83). These structures are depicted in the midcoronal plane at the level of the foramina of Monro (1, 3, and 7 in Fig 2A), where the insular region develops from a U-shape to a T-shape with closure of the interopercular opening (Fig 3). This plane allows minimal variation in ventral or dorsal displacement of the ultrasound probe, is easily identified, and offers the additional advantage of comparing measurements of the left and right hemispheres in a single view. On the basis of the analysis of the 25th and 75th percentiles (Fig 4) and of ROC curves with the Youden index, cutoff values
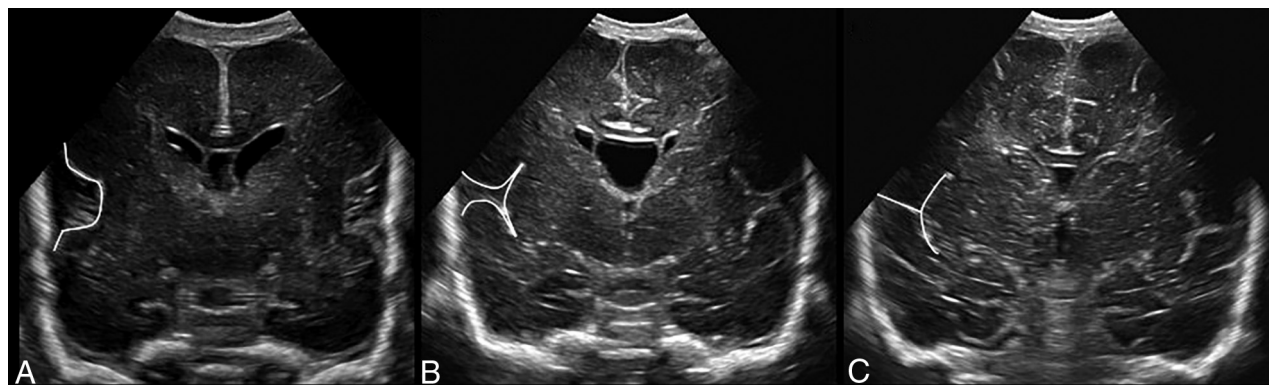
FIG 3. Progression of opercularization with lengthening of insular cortex and closure of interopercular opening in the midcoronal view at different PMAs. *A*, PMA 22 + 6/7 weeks. *B*, PMA 30 + 0/7 weeks. *C*, PMA 34 + 2/7 weeks.
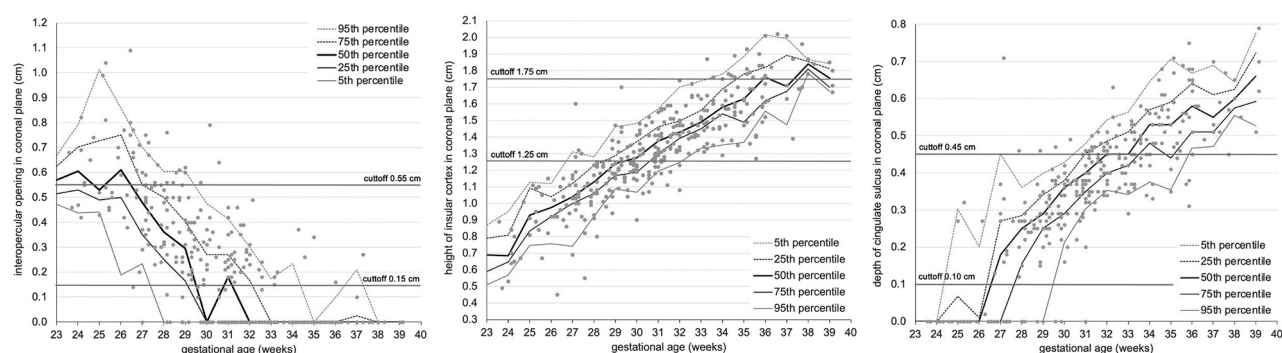

FIG 4. Scatterplot of measurements of selected structures for the USBD and trajectories with 25th and 75th percentiles, regression curves, and selected cutoff values for USBD marked as *lines*. *A*, Interopercular opening. *B*, Height of insular cortex. *C*, Depth of cingulate sulcus in the midcoronal plane.

for the selected structures at a given PMA were identified. Each individual structure could then be scored from 0 to 2, adding to a total score of 0–6 (Table 3).

Cutoff Points for the Interopercular Opening. One scan could not be evaluated for the interopercular opening due to suboptimal image quality. Only 10 infants were scanned at younger than 25 weeks, with greater variability between measurements. Cutoff points for this age range could not be reliably analyzed using ROC curves. The interopercular opening is the only one of the 3 structures suitable for separation at an early PMA because the cingulate sulcus is not visible yet and the height of the insular cortex is not well-defined due to its U-shape. Seventy percent of the infants at a PMA below 25 weeks had an interopercular opening of ≥0.55 cm. A score point of 0 was therefore assigned to infants with an interopercular opening of ≥0.55 cm, which applied to 45 of 343 scans.

Complete closure of the Sylvian fissure was defined as an interopercular opening of <0.15 cm. Complete closure of the Sylvian fissure was achieved at the 25th percentile in scans from 30 weeks' PMA and at the 75th percentile in scans from 33 weeks' PMA. After closure of the Sylvian fissure, this structure can no longer be used to distinguish different PMAs. An interopercular opening of <0.15 cm identifies infants with a PMA of >30 + 6/7 weeks with a sensitivity of 0.83 and a specificity of 0.76 (J =

Table 3: USBD[a]

Score Points	0	1	2
Interopercular opening (cm)	≥ 0.55	0.15–0.54	< 0.15
Height of insular cortex (cm)	≤ 1.25	1.26–1.74	≥ 1.75
Depth of cingulate sulcus (cm)	< 0.10	0.11–0.44	≥ 0.45

[a] Score points from each structure add to a total score, which can range from a minimum of 0 points to a maximum of 6 points (a higher total score reflects a higher PMA).

0.59). Two score points were assigned to 167 of 343 scans accordingly. A score point of 1 was assigned to the remaining 131 of 343 scans.

Cutoff Points for the Height of the Insular Cortex. Three scans could not be evaluated for the insular cortex due to suboptimal image quality. Growth of the insular cortex to a height >1.25 cm was achieved at the 25th percentile in scans from 29 weeks' PMA and at the 75th percentile in scans from 31 weeks' PMA. The cutoff value of > 1.25 cm accurately identified infants with a PMA of >28 + 6/7 weeks with a sensitivity of 0.90 and a specificity of 0.84 (J = 0.74). In 143 of 341 scans, the height of the insular cortex was ≤1.25 cm, and 0 score points were assigned.

Measurements of ≥1.75 cm were reached at the 25th percentile in scans from 35 weeks' PMA and at the 75th percentile in scans from 38 weeks' PMA. The cutoff value of ≥1.75 cm accurately identified infants with a PMA of >34 + 6/7 weeks with a sensitivity of 0.78 and a specificity of 0.90 (J = 0.68). A score

Table 4: PMA mean and range for each USBD score value

Score	No. of Scans with Score Assigned	PMA (Weeks) (mean)	PMA (Weeks) (range)
0	20	25.8 (SD, 1.4)	23 + 4/7 to 29 + 0/7
1	25	26.9 (SD, 1.6)	23 + 5/7 to 29 + 5/7
2	53	28.9 (SD, 1.3)	25 + 0/7 to 32 + 0/7
3	56	30.4 (SD, 1.5)	27 + 0/7 to 35 + 0/7
4	67	32.1 (SD, 1.6)	27 + 1/7 to 36 + 0/7
5	67	34.4 (SD, 1.9)	30 + 2/7 to 39 + 1/7
6	24	36.1 (SD, 1.6)	33 + 2/7 to 39 + 1/7

point of 2 was assigned to 29 of 341 scans accordingly. A score point of 1 was assigned to the remaining 169 of 341 scans.

Cutoff Points for Depth of the Cingulate Sulcus. Twenty-nine scans could not be evaluated for the cingulate sulcus due to insufficient image quality. The first appearance of the cingulate sulcus (defined as a depth >0.10 cm) was at the 25th percentile in scans from 25 weeks' PMA and at the 75th percentile in scans from 28 weeks' PMA. The cutoff value of 0.10 cm accurately identifies infants with a PMA of >25 + 6/7 weeks with a sensitivity of 0.91 and a specificity of 0.89 (J = 0.80). A score point of 0 was assigned to 43 of 315 scans. Before the appearance of the cingulate sulcus, it cannot be used to discriminate among different PMAs.

A depth of ≥0.45 cm was achieved at the 25th percentile in scans from 31 weeks' PMA and at the 75th percentile in scans from 34 weeks' PMA. The cutoff value of 0.45 cm accurately identifies infants with a PMA above 33 + 6/7 weeks with a sensitivity of 0.89 and a specificity of 0.78 (J = 0.67). A score point of 2 was assigned to 110 of 315 scans accordingly. A score point of 1 was assigned to 162 of 315 scans.

In summary, the selected cutoff points should separate infants at approximately 24 and 30 weeks' PMA by the interopercular opening, at 28 and 34 weeks' PMA by the height of the insular cortex, and at 25 and 33 weeks' PMA by the depth of the cingulate sulcus.

Total Score Points in the Final USBD. A total USBD could be calculated in 312 of 344 scans. Table 4 lists means, SDs, and ranges of PMA for each score point of the USBD. To identify the potential impact of postnatally altered brain maturation compared with intrauterine life, we conducted a sensitivity analysis including only scans on DOL 1–3 at a PMA of ≤32 weeks at the time of scan. In 90 scans that fulfilled these criteria, no infant scored 5 or 6 and only 6 infants reached a score of 4 (mean PMA= 31.2 [SD, 0.9] weeks; range = 29 + 4/7 to 32 + 1/7 weeks).

Correlation of USBD and PMA. The USBD correlated significantly with PMA (R = 0.88, P < .001, Fig 5). The USBD increases by 0.43 (95% CI, 0.41–0.46) points per 1 week increase of PMA. Contrariwise, a 1-point increase of the USBD reflects 1.8 weeks or 12.6 days of increase in PMA (95% CI, 1.66–1.87) until the USBD reaches a maximal value of 6 at a mean PMA of 36.1 [SD, 1.6] weeks. In the sensitivity analysis of scans on DOL 1–3, we found a similar correlation (R = 0.76, P < .001) and an 0.41-point increase of the USBD per 1-week increment of PMA (95% CI, 0.33–0.48). A 1-point increase in the USBD reflects 1.4 weeks or 10 days of increase in PMA (95% CI, 1.17–1.68).

DISCUSSION

This study presents the development of a novel bedside ultrasound scoring system for assessing brain maturation in very preterm infants. Currently, in clinical practice, this result is achieved only through subjective estimation. We identified 3 easily measurable landmark structures in a standard transfontanellar midcoronal plane, each exhibiting distinct phases of maturation: the interopercular opening, the height of the insular cortex, and the depth of the cingulate sulcus. By combining thresholds for measurements of these 3 structures into a single score, we achieved reliable discrimination of brain maturation with a precision of approximately 2 weeks' PMA per 1-point increase of the score. The developmental stages observed in this study align with the existing literature, though very few ultrasound studies on postnatal cerebral development in preterm infants have focused on sulcal development and opercularization.[7,24,25]

In our cohort, closure of the Sylvian fissure occurred at a mean PMA of 32.1 (SD, 2.3) weeks, which concurs with the anatomic study by Goldstein et al[26] demonstrating closure of the middle operculum at 32–35 weeks and completed development of the Sylvian fissure at a PMA of 32.5 weeks.

We observed the first visibility of the cingulate sulcus at a mean PMA of 26.5 (SD, 1.8) weeks, with the 25th and 75th percentile at 25 and 28 weeks. In prenatal ultrasound studies,[2,18] the first shallow indentation was found slightly earlier at a mean PMA of 24 weeks, with the 25th and 75th percentiles at 23 and 26 weeks. Our findings are consistent with those of Slagle et al,[25] who described the first appearance on postnatal ultrasound at a mean of 26 weeks and an increasing depth in the midcoronal view with gestational age. Ruoss et al[22] reported the first visibility of the cingulate sulcus in early postnatal MR imaging at a higher PMA around 28–33 weeks.

Antonio et al[27] suggested that assessing the cingulate sulcus and structures on the lateral surface on the brain, particularly opercularization forming the Sylvian fissure, provides reliable indicators of PMA. Our choice of these 3 structures for measurements is further supported by Murphy et al,[24] who demonstrated that the sulci with the most distinctive and consistent changes with advancing PMA were the cingulate sulcus in the midsagittal plane and the closure and infolding of the lateral sulcus in the midcoronal plane.

Incorporating these 3 robust measurements into a single score and dividing the score categories into easily memorizable thresholds offer the potential for this score to become a useful bedside tool for assessing the state of brain maturation with reasonable accuracy. The USBD exhibits a linear relationship with PMA from 22 to 36 weeks' PMA. On reaching its maximum value of 6 around 36 weeks PMA, it is no longer suitable for describing further brain development.

The score was developed in infants without acquired or congenital brain anomalies, limiting its routine use in preterm infants with these conditions. Nonetheless, the USBD can be applied for both cross-sectional and longitudinal ultrasound purposes in premature infants, independent of growth trajectories and percentiles for each individual structure. Longitudinal measurements could provide valuable early bedside evidence of delayed cerebral development resulting from postnatal complications during this vulnerable period of rapid brain maturation. This result has already been demonstrated in intrauterine studies of Sylvian fissure and
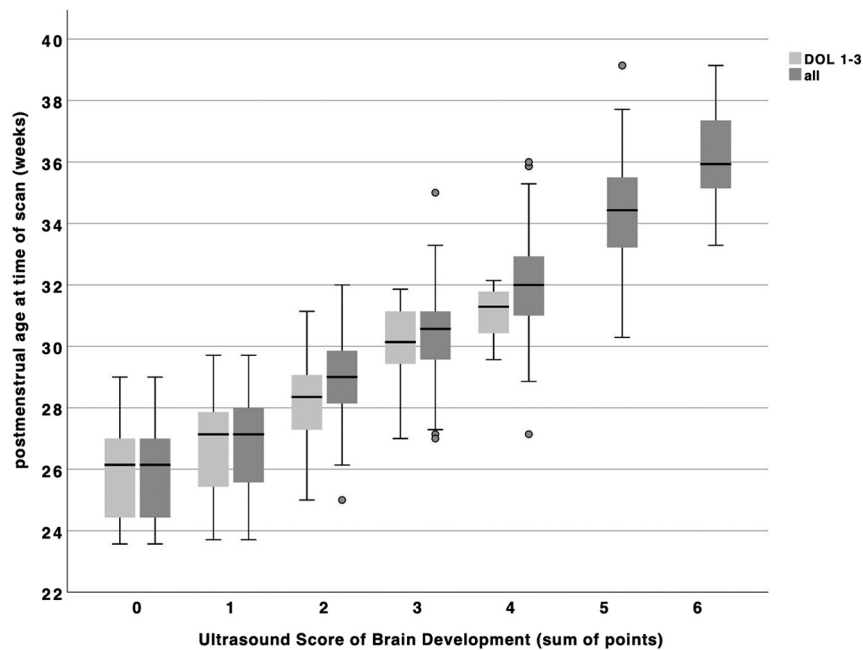
FIG 5. Boxplot of USBD score points by postmenstrual age grouped by day of scan: light gray including only scorable scans from DOL 1–3 (n = 88); dark gray including all scorable scans (n = 312).

cingulate sulcus development, which are components of the USBD.

A major limitation of our study was its retrospective design, which relied on the quality of archived ultrasound scans. Thirty-two scans had to be excluded from analysis because they were not performed specifically for measuring and symmetric visualization of the selected structures. This exclusion specifically limited the interpretation of the first appearance of the cingulate sulcus and therefore calculation of the USBD. We included only preterm infants born at or below 32 weeks' PMA because they are routinely monitored by a standard ultrasound protocol.

The number of scans at earlier than 25 weeks' PMA was limited and exhibited considerable variability in measurements. To increase the total number of available scans, we included serial scans from infants because the number of suitable patients was limited due to the single-center design. However, the correlation of the 3 selected structures as well as the USBD with PMA remained significant when only scans from DOL 1–3 were analyzed. Inter- and intrarater reproducibility and validity of the proposed scoring system should be determined in future prospective studies. These studies should encompass a more diverse cohort, including a larger number of infants with higher and lower PMAs at birth. Application of the USBD in different cohorts of infants with cerebral injury or other insults with an effect on cerebral development will assess its suitability for early bedside detection of disturbances in brain development.

CONCLUSIONS

This study introduces a novel, pragmatic bedside ultrasound scoring system to assess brain maturation in very preterm infants. By incorporating measurements of 3 easily identifiable landmark structures in a single ultrasound plane, our scoring system achieves reliable discrimination of brain maturation with a precision of approximately 2 weeks' PMA. The developmental stages observed are consistent with the existing literature. This scoring system has the potential to become a useful bedside tool for accurately assessing brain maturation in preterm infants.

REFERENCES

1. Achiron R, Achiron A. **Development of the human fetal corpus callosum: a high-resolution, cross-sectional sonographic study.** *Ultrasound Obstet Gynecol* 2001;18:343–47 CrossRef Medline
2. Cohen-Sacher B, Lerman-Sagie T, Lev D, et al. **Sonographic developmental milestones of the fetal cerebral cortex: a longitudinal study.** *Ultrasound Obstet Gynecol* 2006;27:494–502 CrossRef Medline
3. Harreld JH, Bhore R, Chason DP, et al. **Corpus callosum length by gestational age as evaluated by fetal MR imaging.** *AJNR Am J Neuroradiol* 2011;32:490–94 CrossRef Medline
4. Cignini P, Padula F, Giorlandino M, et al. **Reference charts for fetal corpus callosum length: a prospective cross-sectional study of 2950 fetuses.** *J Ultrasound Med* 2014;33:1065–78 CrossRef Medline
5. Koning IV, Roelants JA, Groenenberg IAL, et al. **New ultrasound measurements to bridge the gap between prenatal and neonatal brain growth assessment.** *AJNR Am J Neuroradiol* 2017;38:1807–13 CrossRef Medline
6. Rodriguez-Sibaja MJ, Villar J, Ohuma EO, et al. **Fetal cerebellar growth and Sylvian fissure maturation: international standards from Fetal Growth Longitudinal Study of INTERGROWTH-21st Project.** *Ultrasound Obstet Gynecol* 2021;57:614–23 CrossRef Medline
7. Klebermass-Schrehof K, Moerth S, Vergesslich-Rothschild K, et al. **Regional cortical development in very low birth weight infants with normal neurodevelopmental outcome assessed by 3D-ultrasound.** *J Perinatol* 2013;33:533–37 CrossRef Medline
8. Klebermass-Schrehof K, Aumuller S, Goeral K, et al. **Biometry of the corpus callosum assessed by 3D ultrasound and its correlation to neurodevelopmental outcome in very low birth weight infants.** *J Perinatol* 2017;37:448–53 CrossRef Medline

9. Benavente-Fernández I, Rodríguez-Zafra E, León-Martínez J, et al. **Normal cerebellar growth by using three-dimensional US in the preterm infant from birth to term-corrected age**. *Radiology* 2018;288:254–61 CrossRef Medline

10. Cuzzilla R, Spittle AJ, Lee KJ, et al. **Postnatal brain growth assessed by sequential cranial ultrasonography in infants born <30 weeks' gestational age**. *AJNR Am J Neuroradiol* 2018;39:1170–76 CrossRef Medline

11. Wu PM, Shih HI, Yu WH, et al. **Corpus callosum and cerebellar vermis size in very preterm infants: relationship to long-term neurodevelopmental outcome**. *Pediatr Neonatol* 2019;60:178–85 CrossRef Medline

12. Huang HC, Chou HC, Tsao PN, et al. **Linear growth of corpus callosum and cerebellar vermis in very-low-birth-weight preterm infants**. *J Formos Med Assoc* 2020;119:1292–98 CrossRef Medline

13. Aisa MC, Barbati A, Gerli S, et al. **Brain 3D-echographic early predictors of neuro-behavioral disorders in infants: a prospective observational study**. *J Matern Fetal Neonatal Med* 2022;35:642–50 CrossRef Medline

14. Arena R, Gallini F, De Rose DU, et al. **Brain Growth Evaluation Assessed with Transfontanellar (B-GREAT) ultrasound: old and new bedside markers to estimate cerebral growth in preterm infants—a pilot study**. *Am J Perinatol* 2022 Jan 4 [Epub ahead of print] CrossRef Medline

15. Teli R, Hay M, Hershey A, et al. **Postnatal microstructural developmental trajectory of corpus callosum subregions and relationship to clinical factors in very preterm infants**. *Sci Rep* 2018;8:7550 CrossRef Medline

16. Thompson DK, Inder TE, Faggian N, et al. **Characterization of the corpus callosum in very preterm and full-term infants utilizing MRI**. *Neuroimage* 2011;55:479–90 CrossRef Medline

17. Husen SC, Koning IV, Go A, et al. **Three-dimensional ultrasound imaging of fetal brain fissures in the growth restricted fetus**. *PLoS One* 2019;14:e0217538 CrossRef Medline

18. Pistorius LR, Stoutenbeek P, Groenendaal F, et al. **Grade and symmetry of normal fetal cortical development: a longitudinal two- and three-dimensional ultrasound study.** *Ultrasound Obstet Gynecol* 2010;36:700–08 CrossRef Medline

19. Quarello E, Stirnemann J, Ville Y, et al. **Assessment of fetal Sylvian fissure operculization between 22 and 32 weeks: a subjective approach.** *Ultrasound Obstet Gynecol* 2008;32:44–49 CrossRef Medline

20. Paules C, Miranda J, Policiano C, et al. **Fetal neurosonography detects differences in cortical development and corpus callosum in late-onset small fetuses.** *Ultrasound Obstet Gynecol* 2021;58:42–47 CrossRef Medline

21. Welling MS, Husen SC, Go A, et al. **Growth trajectories of the human fetal brain in healthy and complicated pregnancies and associations with neurodevelopmental outcome in the early life course.** *Early Hum Dev* 2020;151:105224 CrossRef Medline

22. Ruoss K, Lövblad K, Schroth G, et al. **Brain development (sulci and gyri) as assessed by early postnatal MR imaging in preterm and term newborn infants**. *Neuropediatrics* 2001;32:69–74 CrossRef Medline

23. van der Knaap MS, van Wezel-Meijler G, Barth PG, et al. **Normal gyration and sulcation in preterm and term neonates: appearance on MR images**. *Radiology* 1996;200:389–96 CrossRef Medline

24. Murphy NP, Rennie J, Cooke RW. **Cranial ultrasound assessment of gestational age in low birthweight infants**. *Arch Dis Child* 1989;64:569–72 CrossRef Medline

25. Slagle TA, Oliphant M, Gross SJ. **Cingulate sulcus development in preterm infants**. *Pediatr Res* 1989;26:598–602 CrossRef Medline

26. Goldstein IS, Erickson DJ, Sleeper LA, et al. **The lateral temporal lobe in early human life**. *J Neuropathol Exp Neurol* 2017;76:424–38 CrossRef Medline

27. Antonio GE, Chu WC, Yeung DK, et al. **Imaging of the developing brain**. *Neuroembryol Aging* 2008;5:23–31 CrossRef